Published in final edited form as:
Cell Metab. 2014 April 1; 19(4): 630–641. doi:10.1016/j.cmet.2014.03.011.

Proteolytic cleavage of Opa1 stimulates mitochondrial inner membrane fusion and couples fusion to oxidative phosphorylation

Prashant Mishra[1], **Valerio Carelli**[3], **Giovanni Manfredi**[4], and **David C. Chan**[1,2,*]

[1]Division of Biology and Biological Engineering, California Institute of Technology, Pasadena, CA 91125, USA

[2]Howard Hughes Medical Institute, California Institute of Technology, Pasadena, CA 91125, USA

[3]IRCCS Istituto delle Scienze Neurologiche di Bologna, Department of Biomedical and NeuroMotor Sciences, University of Bologna, Via Ugo Foscolo 7, 40123 Bologna, Italy

[4]Departments of Neurology and Neuroscience, Weill Medical College of Cornell University, 1300 York Avenue, A501, New York, NY 10065, USA

SUMMARY

Mitochondrial fusion is essential for maintenance of mitochondrial function. The mitofusin GTPases control mitochondrial outer membrane fusion, whereas the dynamin-related GTPase Opa1 mediates inner membrane fusion. We show that mitochondrial inner membrane fusion is tuned by the level of oxidative phosphorylation (OXPHOS), whereas outer membrane fusion is insensitive. Consequently, cells from patients with pathogenic mtDNA mutations show a selective defect in mitochondrial inner membrane fusion. In elucidating the molecular mechanism of OXPHOS-stimulated fusion, we uncover that real-time proteolytic processing of Opa1 stimulates mitochondrial inner membrane fusion. OXPHOS-stimulated mitochondrial fusion operates through Yme1L, which cleaves Opa1 more efficiently under high OXPHOS conditions. Engineered cleavage of Opa1 is sufficient to mediate inner membrane fusion, regardless of respiratory state. Proteolytic cleavage therefore stimulates the membrane fusion activity of Opa1, and this feature is exploited to dynamically couple mitochondrial fusion to cellular metabolism.

INTRODUCTION

Within a cell, the mitochondria exist as a population of dynamic organelles that continually interact through fusion and fission (Chan, 2012; Westermann, 2010; Youle and van der Bliek, 2012). These opposing processes underlie mitochondrial dynamics and serve to maintain the quality of the mitochondrial population. Mitochondrial dynamics has important

*To whom correspondence should be addressed. dchan@caltech.edu.

roles in mitochondrial DNA (mtDNA) stability, respiratory capacity, apoptosis, response to cellular stress, and mitophagy. Mitochondrial fusion is therefore likely to be regulated by cellular physiology, but this issue is poorly understood.

Mitochondrial fusion requires coordination of outer membrane (OM) and inner membrane (IM) fusion. OM and IM fusion normally occur in unison *in vivo*, but can be experimentally uncoupled (Malka et al., 2005; Meeusen et al., 2004; Meeusen et al., 2006). OM fusion requires the mitofusins Mfn1 and Mfn2, membrane-bound GTPases located on the OM. IM fusion requires the dynamin-related GTPase Opa1 (Meeusen et al., 2006; Song et al., 2009). Each Opa1 splice form (Delettre et al., 2001) encodes an Opa1 precursor that is imported into the mitochondrion, where the N-terminal mitochondrial targeting sequence is removed to produce a long isoform of Opa1 (l-Opa1) embedded in the IM. At steady state, about half of Opa1 exists as l-Opa1, with the remainder cleaved at S1 or S2 sites to create short forms (s-Opa1) that are no longer membrane-anchored (Ishihara et al., 2006). The Oma1 protease is required for S1 cleavage, which occurs at basal levels but can be dramatically induced by depolarization of mitochondria (Ehses et al., 2009; Head et al., 2009). The Yme1L protease is involved in cleavage at S2 (Griparic et al., 2007; Song et al., 2007). A combination of long and short Opa1 isoforms is necessary for fusion (DeVay et al., 2009; Herlan et al., 2003; Song et al., 2007).

Cellular bioenergetics affects mitochondrial dynamics, but this relationship is understood only in vague terms and complicated by conflicting data. Mitochondrial fusion *in vitro* requires ATP or an energy regenerating system (Hoppins et al., 2011; Meeusen et al., 2004; Schauss et al., 2010), but the basis of this requirement is unclear. Some mammalian cells have been reported to respond to galactose medium by enhancing mitochondria tubulation over a period of 2 weeks (Rossignol et al., 2004), but it is unknown whether this morphology change reflects an increase in fusion or a decrease in fission. Moreover, other cell types appear to have no response (Rossignol et al., 2004). Some mammalian cells with OXPHOS defects contain fragmented mitochondria (Koopman et al., 2005; Kwong et al., 2007; Sauvanet et al., 2010), and yeast cells with defective mtDNA show reduced mitochondrial fusion (Sauvanet et al., 2012). It is unknown whether these changes are direct or indirect consequences of mitochondrial dysfunction. However, there are also well-documented cases of patient cells with OXPHOS defects that have no apparent change in mitochondrial morphology (Guillery et al., 2008a; Handran et al., 1997; Huckriede et al., 1995; Sauvanet et al., 2010). In addition, some mitochondrial fusion does proceed in mammalian or yeast cells entirely lacking mtDNA (ρ^0 cells), indicating that mitochondrial fusion can occur in the absence of OXPHOS (Hermann et al., 1998; Legros et al., 2002). These disparate observations do not suggest a simple relationship between OXPHOS activity and mitochondrial fusion.

To resolve these issues, we studied the dependence of mitochondrial fusion on the respiratory activity of mitochondria *in vitro* and *in vivo*. Using an *in vitro* fusion assay with isolated mitochondria, we find that OXPHOS stimulates the coupling between OM and IM fusion. This regulatory mechanism extends to live cells, and patient cells with mtDNA mutations show a selective defect in IM fusion. In the course of identifying the molecular basis for this regulation, we discovered that ongoing cleavage of l-Opa1 stimulates IM

fusion. OXPHOS upregulates IM fusion by enhancing Opa1 cleavage by Yme1L. Indeed, by artificially activating Opa1 cleavage, we can trigger inner membrane fusion *in vitro*. These results indicate that dynamin-related proteins can be activated for membrane fusion by proteolysis and provide a molecular link between cellular metabolism and mitochondrial fusion.

RESULTS

Oxidative culture conditions promote mitochondrial elongation

Given the central role of mitochondria in energy production, we speculated that mitochondrial dynamics might be responsive to cellular metabolism. We used 96-well oxygen consumption measurements to identify specialized media formulations that robustly affect the respiratory activity of mitochondria in cultured mouse embryonic fibroblasts (MEFs). Starting with pyruvate-lacking media with a moderate concentration (10 mM) of glucose, we found that a switch to media containing galactose or ketone bodies (acetoacetate) as the carbon source results in a 1.5–2 fold increase in mitochondrial respiration within 30 minutes (Figure 1A). At this early time, there are no changes in mitochondrial morphology, but by 24 hours a dramatic restructuring is apparent. Whereas cells maintained in customized glycolytic (glucose-containing) media show mostly fragmented and short tubular mitochondria, cells shifted to oxidative media (galactose or acetoacetate) display an increase in long tubular mitochondria (Figure 1B, C). Conversely, shifting cells from glucose-free media to glycolytic media results in a rapid reduction in respiratory activity that is accompanied by a dramatic shortening of mitochondrial length over 24 hours (Figure S1A–C). *Mfn1*-null cells show an increase in respiration in oxidative media but do not elongate their mitochondria (Figure S1D–F), indicating that the rise in respiration is a primary response that is not due to a morphology change. The elongation is not associated with changes in the levels of fusion and fission machinery components (Figure S1G), nor mitochondrial accumulation or phosphorylation of Drp1 (key component of the fission machinery), mechanisms previously shown (Cereghetti et al., 2008; Cribbs and Strack, 2007) to regulate fission (Figure S1H, I).

IM fusion *in vitro* is tuned by OXPHOS activity

To directly probe the relationship between OXPHOS and mitochondrial fusion, we turned to an *in vitro* fusion assay involving isolated organelles (Figure 2A). Mitochondrial fusion is a multistep process consisting of outer membrane (OM) fusion followed by inner membrane (IM) fusion (Meeusen et al., 2004). We developed an *in vitro* fusion assay with a fluorescent readout that allows these steps to be resolved. Mitochondria were separately isolated from two cell lines stably expressing fluorescent submitochondrial markers. One cell line expressed GFP targeted to the OM membrane and CFP targeted to the matrix; the other expressed RFP targeted to the matrix. This combination of markers allows facile scoring of both OM and IM fusion events simultaneously in a single reaction after mixing (Figure 2B, S2A). Full fusion events are defined by coupled OM and IM fusion and result in complete colocalization of CFP and RFP fluorescence, which are surrounded by a single GFP-labeled membrane (Figure S2B). OM events that do not progress to IM fusion result in neighboring CFP and RFP compartments that are surrounded by a single GFP labeled OM (Figure S2C).

With optimal reaction conditions (see later), greater than 20% of the mitochondria show full fusion, with very few intermediates trapped at the initial stage of OM fusion (Figure 2C). This fusion assay shows several expected features: OM fusion depends on both GTP hydrolysis and mitofusins, whereas IM fusion requires Opa1 (Figure S2D, E).

We found that efficient coupling of OM and IM fusion requires the presence of respiratory substrates, such as succinate and ADP for respiration via complex II of the electron transport chain (ETC) (Figure 2C). When both substrate and ADP are supplied, >95% of OM fusion events culminate in IM fusion. These conditions correspond to state 3 respiration (Chance and Williams, 1955), where substrate and ADP are not limiting, and the electron transport chain is highly active. In contrast, when both succinate and ADP are absent, OM fusion proceeds at normal levels but is completely uncoupled from IM fusion (Figure 2C). When only ADP or succinate is omitted, about half of the OM fusion events progress to full fusion. This effect is probably due to low levels of endogenous ADP and substrate present in the mitochondrial preparations. Consistent with this idea, pre-incubation of mitochondria with ADP to deplete endogenous substrate abolishes this effect (Figure S2F).

These reconstitution data suggest that OXPHOS rates can control mitochondrial fusion efficiency at the level of IM fusion. Oxygen consumption measurements indicated that our isolated mitochondria are highly active, intact, and responsive to pharmacologic inhibition of the ETC (Figure S2G, H). We therefore tested the effect of OXPHOS inhibition on OM and IM fusion. With the complex II substrate succinate, inhibition of ETC complex II, III, IV, or of the ATP synthase (complex V) potently blocks IM fusion but leaves OM fusion intact (Figure 2D). The inhibitory effect of the complex II inhibitor atpenin A5 can be bypassed by driving the ETC via complex I with pyruvate and malate. Analogously, the complex I inhibitor rotenone potently blocks IM fusion driven by complex I substrates (pyruvate/malate) but does not inhibit fusion driven by succinate. In contrast, OM fusion occurs at normal levels in mitochondria with impaired OXPHOS.

We tested whether inactivation of Opa1 via enhanced processing might be responsible for the sensitivity of IM fusion to respiration inhibition. Loss of membrane potential through the addition of uncouplers (e.g., CCCP) causes inactivation of Opa1 via complete cleavage of the long form (Duvezin-Caubet et al., 2006; Ishihara et al., 2006) by the protease Oma1 (Ehses et al., 2009; Head et al., 2009). In our *in vitro* fusion reactions, CCCP induced efficient cleavage of Opa1 to short isoforms as expected (Figure S2I). In contrast, pharmacologic inhibition of OXPHOS or the lack of respiratory substrates did not cause such aberrant Opa1 processing (Figure S2I, J). Thus, the sensitivity of IM fusion to respiration is not a consequence of proteolytic inactivation of Opa1. In addition, mitochondrial membrane potential does not appear to be the key factor, because oligomycin treatment results in loss of IM fusion despite hyperpolarization of the mitochondria (Figure S2K).

The ultimate function of the electron transport chain is to drive formation of ATP in the mitochondrial matrix via complex V activity. When ATP is added to the fusion reaction in the absence of respiratory substrates, we obtained a partial rescue of IM fusion (Figure 2E). This effect was not due to a stimulation of OXPHOS, via contaminating ATPases that may

generate ADP (Figure S2L). Similarly, production of ATP via induction of substrate level phosphorylation in the tricarboxcylic acid (TCA) cycle partially rescues IM fusion in the absence of respiratory substrates (Figure 2E).

Taken together, these data reveal two important features of mitochondrial fusion *in vitro*. First, OM fusion is highly active as long as mitofusins and GTP are present. Second, ETC activity can stimulate mitochondrial IM fusion *in vitro*. To extend this latter concept, we tested whether the activity of the ETC might directly tune the levels of mitochondrial fusion. By systematically varying the availability of respiratory substrates *in vitro*, we found that the IM fusion rate closely correlates with oxygen consumption, whereas OM fusion is insensitive (Figure 2F, S2M).

IM fusion in cultured cells can be controlled by OXPHOS activity

To test whether these *in vitro* insights apply to intact cells, we measured mitochondrial fusion in cells as a function of respiration. Utilizing a photoactivatable GFP (PA-GFP) targeted to either the OM or matrix, we measured OM and IM fusion rates respectively by following the decline in PA-GFP intensity due to fusion (Figure 3). Consistent with our *in vitro* results, OM fusion rates are statistically indistinguishable in glycolytic versus oxidative media, whereas IM fusion rates increase in oxidative media (Figure 3A–C). This increase in IM fusion is apparent at 1–2 hours after the media shift, well before any obvious change in the steady state morphology of mitochondria. Similarly, inhibition of OXPHOS by the complex III inhibitor antimycin A causes a prominent decrease in IM fusion efficiency with no observable effect on OM fusion (Figure 3D).

By tracking individually labeled mitochondria, we could directly visualize the coupling of OM and IM fusion (Figure S3). In customized glycolytic media, 38% of OM fusion events did not immediately proceed to IM fusion (28 of 74). In contrast, in oxidative media, only 7% of OM fusions events (5 of 70) did not proceed to IM fusion. Thus, OXPHOS activity has a selective effect on the IM fusion efficiency. Under glycolytic conditions, many OM fusion events are uncoupled from IM fusion. These events were subsequently resolved by either fission or a 1–2 minute delay in IM fusion (Figure S3B, C). Therefore, uncoupling of OM fusion from IM fusion can occur under physiological conditions. Because nonproductive OM fusion intermediates are resolved by fission, the uncoupling rate can regulate the overall fusion rate of the matrix compartment.

Mitochondrial encephalomyopathies cause a selective defect in IM fusion

Genetic defects in the OXPHOS machinery cause mitochondrial encephalomyopathies (DiMauro and Schon, 2003) that are associated with defective mitochondrial ATP production, as well as muscular and nervous system pathology. Our findings above suggest that mitochondrial IM fusion rates may be depressed in these patients, especially under oxidative conditions. To test this hypothesis, we used isogenic cybrid cell lines harboring homoplasmic mtDNA mutations derived from patients with mitochondrial encephalomyopathy. The “ND1” cell line has severely reduced complex I activity, with no effect on complex II driven respiration (Baracca et al., 2005). The “COXI” cell line is defective in complex IV and therefore has no measurable respiration via either complex I or

complex II (Kwong et al., 2007). When grown in glucose-containing media, these two mutant cell lines have mitochondrial morphologies that are indistinguishable from that of wildtype cells (Figure 4A, B). Upon transfer to oxidative media, however, mutant cells are severely defective in mitochondrial elongation.

To quantify intrinsic mitochondrial fusion rates, we returned to the *in vitro* fusion assay. Mitochondria from ND1 and COXI mutant cells exhibit a specific defect in IM fusion, with no reduction of OM fusion rates (Figure 4C). Importantly, the IM fusion defect of ND1 mitochondria, but not COXI mitochondria, can be fully rescued by driving OXPHOS with complex II substrates. In addition, both cell lines show normal levels of IM fusion driven by substrate level phosphorylation. Therefore, these disease cells have no intrinsic defect in the mitochondrial fusion machinery but have a specific defect in OXPHOS-driven mitochondrial fusion.

Proteolytic cleavage of Opa1 is required for OXPHOS-stimulated fusion

To understand the molecular basis of OXPHOS-induced membrane fusion, we screened for pharmacologic agents that specifically inhibit this process. Numerous compounds--including kinase and phosphatase inhibitors, deacetylase inhibitors, and oxidizing and reducing agents--had no effect on inner or outer membrane fusion (Figure S4A). The metalloprotease inhibitor o-phenanthroline, however, completely blocked inner membrane fusion while leaving outer membrane fusion intact (Figure 5A). This inhibitory effect was not due to an inhibition of respiration (Figure S4B) and could not be rescued by addition of ATP, suggesting the ATP may work upstream of the step inhibited by o-phenanthroline.

Intriguingly, Opa1, the central protein involved in IM fusion, is proteolytically processed by two metalloproteases, Oma1 and Yme1L. Oma1 processes l-Opa1 at the S1 cleavage site, whereas Yme1L processes l-Opa1 isoforms containing the S2 cleavage site (Figure 5B). Oma1 activity is inhibited by o-phenanthroline (Ehses et al., 2009; Kaser et al., 2003), and Yme1L belongs to a family of zinc-binding proteases (Langklotz et al., 2012) that should also be inhibited by metal chelation. These observations suggest the possibility that ongoing Opa1 cleavage is required for IM fusion. If this idea is correct, cleavage events should accumulate during the course of a productive fusion reaction. We measured cleavage at S1 in mitochondria containing Myc-tagged Opa1 isoform 1 (which only contains the S1 site), and cleavage at S2 in mitochondria containing Opa1 isoform 7ΔS1 (which only contains the S2 site). Processing at S2 was stimulated by respiratory substrates or ATP (Figure 5C), conditions which promote IM fusion. This stimulation was eliminated by the OXPHOS inhibitors antimycin A and oligomycin and by o-phenanthroline (Figure 5D). Thus, cleavage at S2 correlates with mitochondrial IM fusion *in vitro*. S1 cleavage was not stimulated by conditions permissive for IM fusion (Figure 5C). We observed similar stimulation of S2 (but not S1) cleavage in cells cultured under oxidative conditions (Figure S4C, D). Consistent with a role for S2 cleavage, cells containing mtDNA mutations in ND1 or COX1 show a selective reduction in S2 cleavage products (Figure S4E).

To further define the genetic requirements for OXPHOS-stimulated fusion, we examined cells lacking Oma1 or Yme1L. Like wildtype cells, *Oma1*-null MEFs respond to respiratory conditions by mitochondrial elongation (Figure S5A, B). In contrast, knockdown of Yme1L

(Figure 6A, B, S5C) prevents mitochondrial elongation induced by oxidative media, despite a normal mitochondrial respiration response (Figure S5D). This defect was rescued by expression of an RNAi-resistant form of Yme1L (Figure S5E). The inhibition of mitochondrial elongation is due to a failure to stimulate inner membrane fusion under oxidative conditions, with no effect on outer membrane fusion (Figure 6C, D, S5F, G). IM fusion rates in glycolytic conditions were unaffected (Figure 6C). To further test the role of Yme1L, we designed siRNAs to selectively remove Opa1 mRNA splice forms that contain exon 5b, which encodes the S2 cleavage site. Two independent siRNAs against exon 5b blocked OXPHOS-stimulated mitochondrial elongation (Figure 6E, F, S5H, I). In contrast, neither Yme1 nor Oma1 was singly required for mitochondrial elongation stimulated by starvation or cycloheximide treatment (Figure S5J).

Proteolytic activation of Opa1 is sufficient to trigger inner membrane fusion

Mitochondrial dysfunction is often associated with increased Opa1 cleavage (Duvezin-Caubet et al., 2006; Guillery et al., 2008b; Ishihara et al., 2006), leading to the idea that Opa1 cleavage inactivates mitochondrial fusion. Our data suggest the opposite hypothesis that real-time proteolysis of Opa1 stimulates fusion. To expand this idea, we asked whether artificial cleavage of Opa1 is sufficient to trigger inner membrane fusion. We used an engineered version of Opa1 with no endogenous cleavage sites (isoform 1ΔS1) (Song et al., 2007) and introduced an artificial cleavage site recognized by the tobacco etch virus (TEV) protease at the position of the S2 site. This Opa1 variant was expressed in *Opa1*-null MEFs, and isolated mitochondria were analyzed in an *in vitro* fusion reaction. Mixed mitochondria were allowed to enter the initial stage of fusion, during which OM fusion occurred. We treated the mitochondria with a low concentration of digitonin that permeabilized the OM but left the IM intact (Figure S6A), and then added TEV protease to the reaction (Figure 7A). Strikingly, addition of digitonin and TEV were sufficient to promote inner membrane fusion events, despite the absence of respiratory substrates and ATP (Figure 7B). Importantly, these events also bypassed the inhibitory effect of o-phenanthroline. Controls indicated that both digitonin and TEV were necessary to activate fusion, and no activation was observed with mitochondria containing an Opa1 variant lacking the TEV site (Figure 7B). Thus, proteolytic cleavage of Opa1 at S2 stimulates inner membrane fusion.

These results prompted us to examine whether cleavage at S1 could similarly stimulate inner membrane fusion. Opa1 splice forms that contain only an S1 site are sufficient to restore mitochondrial fusion to *Opa1*-null cells (Song et al., 2007). Mitochondria containing an Opa1 variant with a TEV site in place of S1 showed inner membrane fusion triggered by digitonin and TEV (Figure 7C). Thus, activation of Opa1 is not limited to the S2 site; cleavage appears to be a general mechanism to stimulate IM fusion.

Treatment of cells or mitochondria with CCCP is known to inactivate mitochondrial fusion by inducing complete l-Opa1 cleavage at S1 by Oma1 (Ehses et al., 2009; Head et al., 2009; Ishihara et al., 2006). As a result, cleavage at S1 induced by CCCP treatment is generally thought to inactivate Opa1 function. In contrast, we wondered whether CCCP treatment might be able to paradoxically stimulate IM fusion of mitochondria stalled after OM fusion by respiratory inhibition. Wild-type mitochondria were allowed to undergo OM fusion *in*

vitro, and then CCCP was added (Figure 7D). Remarkably, CCCP treatment stimulated inner membrane fusion, removing the normal requirement for respiratory substrates (Figure 7E). Unlike OXPHOS-stimulated fusion, the CCCP-induced fusion is resistant to oligomycin treatment. It is, however, abolished by o-phenanthroline (Figure 7E), consistent with the expectation that the CCCP effect is operating via cleavage of Opa1 (Figure S6B). To formally demonstrate the role of Oma1, we examined mitochondrial fusion in *Oma1*-null cells. These cells show normal OXPHOS-stimulated IM fusion (as Yme1L is unaffected), but do not show CCCP-stimulated cleavage of Opa1 (Figure S6C) nor CCCP-stimulated fusion (Figure 7F). Taken together, these data indicate that Yme1L and Oma1 have pro-fusion roles, and that artificial cleavage of Opa1 can bypass the block to IM fusion caused by inhibition of OXPHOS.

DISCUSSION

Previous work defined a requirement for ATP in mitochondrial fusion (Hoppins et al., 2011; Meeusen et al., 2004; Schauss et al., 2010). In this study, we show that beyond having an energy requirement, mitochondrial fusion is sensitive to the OXPHOS activity of mitochondria. By tuning the levels of mitochondrial IM fusion to OXPHOS activity, cells may ensure that mitochondrial morphology and function match energy demands. Because OM fusion is insensitive to changes in mitochondrial metabolism, physiological uncoupling of outer and IM fusion can control overall fusion rates of the mitochondrial matrix. OXPHOS-stimulated inner membrane fusion is disturbed in patients with mitochondrial encephalomyopathies. It should be noted that our *in vitro* assay with isolated mitochondria appears to primarily measure fusion associated with Yme1L-mediated cleavage of Opa1. *In vivo*, we expect Oma1-mediated cleavage to also be important.

Two distinct models have related Opa1 processing to mitochondrial fusion. First, both long and short isoforms are required for membrane fusion (DeVay et al., 2009; Herlan et al., 2003; Song et al., 2007). As a result, some proteolysis of Opa1 at S1 or S2 is required to produce an appropriate ratio of long and short isoforms. However, our results indicate that simply having a normal ratio of long and short isoforms is not sufficient for IM fusion, because mitochondria incubated acutely with o-phenanthroline show normal ratios of long and short Opa1 isoforms but have complete loss of IM fusion. Second, collapse of the mitochondrial inner membrane potential by CCCP induces Oma1-dependent cleavage at S1 sites, complete loss of l-Opa1, and loss of mitochondrial fusion (Ehses et al., 2009; Head et al., 2009; Ishihara et al., 2006). Other conditions that cause mitochondrial dysfunction also promote excessive Opa1 cleavage, leading to the idea that Opa1 cleavage is an anti-fusion mechanism to prevent the merger of compromised mitochondria (Duvezin-Caubet et al., 2006). However, long-term depolarization by CCCP is a nonphysiological condition, and it is difficult to extrapolate the endogenous function of Oma1 cleavage from such experiments.

In contrast to these models, our data argue that proteolysis of Opa1 is a pro-fusion event that operates at the time of fusion (Fig. 7G). Although our study is focused on the bioenergetic regulation of IM fusion, it should be emphasized that Opa1 cleavage appears to be involved regardless of whether fusion is constitutive or regulated. The importance of real-time cleavage of Opa1 during the fusion reaction is strongly supported by our observation that

artificial cleavage of l-Opa1 is sufficient to drive inner membrane fusion. We imagine that Opa1 cleavage triggers structural rearrangements and/or stimulation of GTPase activity to promote the fusion reaction. This process ultimately results in a mixed population of long and short isoforms at steady state. Experiments with Mgm1, the yeast ortholog of Opa1, suggest that the short isoform has enhanced GTPase activity required for fusion (DeVay et al., 2009; Herlan et al., 2003). In a possible scenario, the cleavage of tethered l-Opa1 complexes may stimulate GTPase activity (via production of s-Opa1) and associated conformational changes to drive membrane fusion. Future experiments with cell-free fusion assays will be necessary to determine the molecular details of Opa1 activation. Although we find that Opa1 cleavage stimulates IM fusion, our results do not rule out the possibility that uncleaved Opa1 can mediate a basal level of fusion.

With Opa1 proteolytic cleavage associated with the fusion mechanism, control of the cleavage step provides an opportunity to regulate fusion. The interaction of two inner membrane proteases with Opa1 probably enables its activity to be differentially regulated. With Yme1L (an ATP-dependent protease), OXPHOS or ATP stimulates cleavage of Opa1 at S2, thereby enhancing IM fusion in response to metabolic signals. Indeed, cleavage activity at S2 is lower in cells with pathogenic mtDNA mutations (Figure S4E). It is interesting to note that Yme1L has been reported to interact with subunits of complex V (Stiburek et al., 2012), raising the possibility that it may directly sense ATP-generation by the respiratory chain. Opa1 can also be activated by Oma1-mediated cleavage at S1, although this mechanism is not engaged during OXPHOS-stimulated fusion *in vitro*. Pharmacologic treatment by CCCP is the best-documented activator of Oma1 (Ehses et al., 2009; Head et al., 2009). Interestingly, mitochondria are known to undergo transient depolarizations that correlate with fusion events (Santo-Domingo et al., 2013), and such events may serve to stimulate Oma1 activity under basal conditions.

EXPERIMENTAL PROCEDURES

Reagents

Antibodies to the following proteins were used: Drp1 (BD Biosciences), Drp1 S637-PO_4 (Cell Signaling), Actin (Millipore), Fis1 (Alexis Corps), Mff (Sigma-Aldrich), Mfn1 (Chen et al., 2003), Mfn2 (Sigma), Opa1 (in house monoclonal), ClpP (Proteintech Group), Oxa1 (Proteintech Group), Tom20 (Santa Cruz BioTech), Hsp60 (Santa Cruz BioTech), Yme1L (Proteintech Group), Myc (Covance). Oligomycin (Sigma-Aldrich), antimycin A (Sigma-Aldrich), atpenin A5 (Santa Cruz BioTech), CCCP (Sigma-Aldrich) and atractyloside (Sigma-Aldrich) were used at 1 μM. Concentrations of other compounds: rotenone (Sigma-Aldrich), 200 nM; KCN (Sigma-Aldrich), 1 mM; o-phenanthroline (Sigma-Aldrich), 0.5 mM; aspartate, 1 mM; ADP (Sigma-Aldrich), 200 μM; β-NADH (Sigma-Aldrich), 2 mM. Unless otherwise indicated, substrates (pyruvate, malate, succinate, α-ketoglutarate) were used at 5 mM.

Cell Culture

MEFs (mouse embryonic fibroblasts) were maintained in Dulbecco's Modified Eagle Medium (DMEM) supplemented with 10% fetal bovine serum (FBS), 2 mM L-glutamine,

and penicillin/streptomycin at 37 °C and 5% CO2. 143B (human osteosarcoma) cells were similarly maintained, except with 5% FBS and the addition of 50 μg/mL uridine. *Opa1*-null and *Oma1*-null MEFs were described previously (Quiros et al., 2012; Song et al., 2007). Cells with homoplasmic mtDNA mutations are cybrids from the fusion of enucleated patient cells with 143B rho^0 cells (lacking mtDNA) (Baracca et al., 2005; Kwong et al., 2007). ND1 cells have a G → A mutation at nucleotide 3460 in the ND1 subunit of complex I. COXI cells have a premature stop codon at nucleotide 6390 in the cytochrome *c* oxidase subunit I gene of complex IV. Stable cell lines with labeled mitochondria were generated by retroviral infection. Fluorescent proteins were targeted to either the OM (via fusion with the C-terminus of OMP25) or the matrix (via fusion with the mitochondrial targeting sequence at the N-terminus of COX8). Highly fluorescent clonal populations were selected for use in the *in vitro* mitochondrial fusion assay. Mitochondrial morphology was scored in triplicate with greater than 100 cells per experiment.

To quantify S1 and S2 processing, wild-type MEFs were stably infected with retroviruses encoding either mouse Opa1 isoform 1 (S1 site only), or mouse Opa1 isoform7ΔS1 [S1 site (amino acids 191–201) deleted, S2 site present]. For TEV protease experiments, Opa1-null MEFs were stably infected with retrovirus encoding mouse Opa1 isoform 1ΔS1 (S1 site deleted) with a TEV protease site (GENLYFQ) inserted at either the S1 site (after amino acid 190), or at the S2 (exon 5b; after amino acid 208) site.

shRNAi against Yme1L was performed as described previously (Song et al., 2007). The targeted sequence of Yme1L was GAGTGGCAGAGGAACTCATAT. Infected MEFs were plated at low density to obtain clonal populations with stable knockdown of Yme1L. Yme1L-knockdown cells were rescued by infection with retroviruses encoding RNAi-resistant mouse Yme1L.

siRNA against exon5b of mouse Opa1 was performed using two separate sequences. siRNA oligonucleotides were purchased from Integrated DNA Technologies.

Exon 5b siRNA#1:

Sense: 5′-rGrCrArCrGrArArGrArGrGrArArGrCrArCrGrCrArGrArGdCdC-3′

Antisense: 5′-rGrGrCrUrCrUrGrCrGrUrGrCrUrUrCrCrUrCrUrUrCrGrUrGrCrUrC-3′

Exon 5b siRNA#2:

Sense: 5′-rCrArUrUrCrUrCrUrUrArCrArArCrArGrCrArArArUrUrCdAdA-3′

Antisense: 5′-
rUrUrGrArArUrUrUrGrCrUrGrUrUrGrUrArArGrArGrArArUrGrArG-3′

Here, ‘r’ refers to a ribonucleic base, and ‘d’ refers to a deoxyribonucleic base. siRNA duplexes were transfected into cells at 50 nM using Lipofectamine 2000 (Invitrogen) at the time of cell plating, and again at 24 and 48 hours. Cells were assayed at 72 hours for their ability to respond to oxidative media.

Customized glycolytic and oxidative media were used. The base DMEM solution lacks glucose, pyruvate and glutamine (Invitrogen Catalog #A14430). Glucose-containing

(glycolytic) media: DMEM supplemented with 10% dialyzed FBS, 10 mM glucose, 4 mM glutamine, and penicillin/streptomycin. It should be noted that this glycolytic media is distinct from the standard high-glucose DMEM media used for routine culture of MEFs. Galactose-containing (oxidative) media: DMEM supplemented with 10% dialyzed FBS, 10 mM galactose, 4 mM glutamine, and penicillin/streptomycin. Acetoacetate-containing (oxidative) media: DMEM supplemented with 10% dialyzed FBS, 10 mM acetoacetate, 4 mM glutamine, and penicillin/streptomycin. For media exchanges, cells were washed three times with the indicated media. For starvation experiments, cells were washed three times and incubated in HBSS (Hank's Balanced Salt Solution, Invitrogen Catalog #14025).

Mitochondrial isolation and *in vitro* mitochondrial fusion assay

Mitochondria were isolated from cells via differential centrifugation. Cells were washed and harvested by scraping in isolation buffer (5 mM HEPES, 200 mM mannitol, 70 mM sucrose, 70 mM KCl, 0.5 mM EGTA, 5 mM K_2HPO_4, 1 mM $MgCl_2$, and HALT protease inhibitors) and lysed via nitrogen cavitation (250 psi, 20 min, 4 °C). Lysates were cleared of cell debris and nuclei with four 600 *g* spins. A crude mitochondrial fraction was isolated from the cleared lysate via a 10000 *g* spin and washed three times in isolation buffer.

For the *in vitro* fusion assay, we utilized a procedure similar to previously reported assays (Hoppins et al., 2011; Meeusen et al., 2004; Schauss et al., 2010). Differentially labeled mitochondria were mixed and pelleted at 10000 *g* for 2 min to promote interaction. After 20 min on ice, the pellet was resuspended and incubated at 37 °C for 60 min in the presence of additional additives (e.g., substrate, GTP, ATP, ADP, drugs), and then fixed at room temperature with an equal volume of formalin. Mitochondria were visualized under a fluorescent microscope and scored according to colocalization of different fluorescent proteins as described in the text. Approximately 100–200 mitochondria were counted per reaction; reactions were performed in triplicate.

For the induced cleavage reactions (Figure 7), step 1 (OM fusion only) was performed at 37 °C for 30 min in the presence of the indicated additives. After 30 minutes, additional additives (e.g., digitonin, TEV protease (Invitrogen; 1 unit/reaction), CCCP (1 μM) were added, and the reaction was incubated at 37 °C for an additional 30 min (step 2), followed by fixation and analysis. For proteinase K experiments, mitochondria after step 1 were incubated on ice in the presence of different concentrations of digitonin (0.02–0.1%). Proteinase K was added (final concentration 10 μg/mL), and the reactions were incubated for 10 min on ice. The reaction was stopped by pelleting the mitochondria and resuspending them in lysis buffer (2% SDS, 25 mM Tris pH 6.8) with PMSF supplemented to 1 mM.

In vivo mitochondrial fusion assay

Cells expressing matrix DsRed and photoactivatable GFP (PA-GFP) targeted to either the OM or matrix were plated on glass coverslips and imaged live at 37 °C on an LSM 710 confocal microscope (Carl Zeiss, Inc.). PA-GFP was photoactivated in a region of interest (5 μm × 5 μm) by illumination with a 405 nm laser. The activated fluorescent signal was then collected (for the entire cell) every 3 minutes for the next 30 minutes using a spectral detector, followed by spectral unmixing based on the individual PA-GFP and DsRed

spectra. Fusion events result in the dilution of the activated signal. The average pixel intensity (for the entire cell) over time is a measurement of fusion rates (Karbowski et al., 2004). Images were analyzed in MatLab (Mathworks, Inc.). P-values were calculated using a Students *t*-test on the slopes of intensity versus time for individual measurements (>20 per condition).

To follow individual fusion events, cells expressing matrix DsRed and OM-PA-GFP were imaged on glass coverslips at 37 °C. Simultaneous photoactivation of PA-GFP (with a 405 nm laser) and bleaching of matrix DsRed (with a 561 nm laser) was used to label specific mitochondria. Images were collected (as above) every 20 seconds for 10 min and analyzed manually for fusion events.

Respiration and membrane potential measurements

Oxygen consumption rate was measured in a Seahorse Biosciences Extracellular Flux Analyzer (model XF96). 10,000 cells per well were plated 18 hours prior to measurement in complete medium in a 96-well plate. Four hours prior to measurement, cells were equilibrated in media made with DMEM lacking bicarbonate (Sigma-Aldrich Catalog #D5030). Oxygen levels were measured over 5 minute periods, and media exchange was performed using the XF96 PrepStation (Seahorse Bioscience).

Respiration measurements on isolated mitochondria were performed as previously described (Rogers et al., 2011). Briefly, *in vitro* fusion assays were set up (as described above) in 100 µl reaction volumes. 50 µL (2 µg mitochondrial protein) aliquots of each reaction were placed in a 96-well Seahorse TC plate. The plate was spun at 2000 *g*, 4 °C for 20 min to pellet mitochondria. Additional isolation buffer was added to a final volume of 200 µl. The plate was equilibrated for 10 min at 37 °C prior to measuring oxygen consumption. Oxygen levels were measured over 5 minute periods.

Membrane potential measurements on isolated mitochondria were performed by visualization of TMRM fluorescence. Mitochondria from the indicated condition were loaded with TMRM (10 nM) for 10 minutes at room temperature and then washed into isolation buffer containing 2 nM TMRM. Samples were imaged by fluorescence microscopy using identical imaging parameters. The average fluorescence for each mitochondrion (after subtraction of background fluorescence) was calculated. Greater than 100 mitochondria were quantified per sample, and experiments were performed in triplicate.

Supplementary Material

Refer to Web version on PubMed Central for supplementary material.

Acknowledgments

This work was supported by grant GM062967 from the National Institutes of Health. P.M. was supported by a fellowship from the Jane Coffin Childs Memorial Fund for Medical Research. We thank Dr. Andrea Martinuzzi for construction of the ND1 cybrid, Dr. Carlos López-Otín for providing *Oma1*-null cells, and members of the Chan lab for helpful discussions and comments on the manuscript.

References

Baracca A, Solaini G, Sgarbi G, Lenaz G, Baruzzi A, Schapira AH, Martinuzzi A, Carelli V. Severe impairment of complex I-driven adenosine triphosphate synthesis in leber hereditary optic neuropathy cybrids. Archives of neurology. 2005; 62:730–736. [PubMed: 15883259]

Cereghetti GM, Stangherlin A, Martins de Brito O, Chang CR, Blackstone C, Bernardi P, Scorrano L. Dephosphorylation by calcineurin regulates translocation of Drp1 to mitochondria. Proc Natl Acad Sci U S A. 2008; 105:15803–15808. [PubMed: 18838687]

Chan DC. Fusion and fission: interlinked processes critical for mitochondrial health. Annual review of genetics. 2012; 46:265–287.

Chance B, Williams GR. Respiratory enzymes in oxidative phosphorylation. III. The steady state. J Biol Chem. 1955; 217:409–427. [PubMed: 13271404]

Chen H, Detmer SA, Ewald AJ, Griffin EE, Fraser SE, Chan DC. Mitofusins Mfn1 and Mfn2 coordinately regulate mitochondrial fusion and are essential for embryonic development. J Cell Biol. 2003; 160:189–200. [PubMed: 12527753]

Cribbs JT, Strack S. Reversible phosphorylation of Drp1 by cyclic AMP-dependent protein kinase and calcineurin regulates mitochondrial fission and cell death. EMBO Rep. 2007; 8:939–944. [PubMed: 17721437]

Delettre C, Griffoin JM, Kaplan J, Dollfus H, Lorenz B, Faivre L, Lenaers G, Belenguer P, Hamel CP. Mutation spectrum and splicing variants in the OPA1 gene. Hum Genet. 2001; 109:584–591. [PubMed: 11810270]

DeVay RM, Dominguez-Ramirez L, Lackner LL, Hoppins S, Stahlberg H, Nunnari J. Coassembly of Mgm1 isoforms requires cardiolipin and mediates mitochondrial inner membrane fusion. J Cell Biol. 2009; 186:793–803. [PubMed: 19752025]

DiMauro S, Schon EA. Mitochondrial respiratory-chain diseases. N Engl J Med. 2003; 348:2656–2668. [PubMed: 12826641]

Duvezin-Caubet S, Jagasia R, Wagener J, Hofmann S, Trifunovic A, Hansson A, Chomyn A, Bauer MF, Attardi G, Larsson NG, et al. Proteolytic processing of OPA1 links mitochondrial dysfunction to alterations in mitochondrial morphology. J Biol Chem. 2006; 281:37972–37979. [PubMed: 17003040]

Ehses S, Raschke I, Mancuso G, Bernacchia A, Geimer S, Tondera D, Martinou JC, Westermann B, Rugarli EI, Langer T. Regulation of OPA1 processing and mitochondrial fusion by m-AAA protease isoenzymes and OMA1. J Cell Biol. 2009; 187:1023–1036. [PubMed: 20038678]

Griparic L, Kanazawa T, van der Bliek AM. Regulation of the mitochondrial dynamin-like protein Opa1 by proteolytic cleavage. J Cell Biol. 2007; 178:757–764. [PubMed: 17709430]

Guillery O, Malka F, Frachon P, Milea D, Rojo M, Lombes A. Modulation of mitochondrial morphology by bioenergetics defects in primary human fibroblasts. Neuromuscular disorders : NMD. 2008a; 18:319–330. [PubMed: 18395446]

Guillery O, Malka F, Landes T, Guillou E, Blackstone C, Lombes A, Belenguer P, Arnoult D, Rojo M. Metalloprotease-mediated OPA1 processing is modulated by the mitochondrial membrane potential. Biology of the cell/under the auspices of the European Cell Biology Organization. 2008b; 100:315–325. [PubMed: 18076378]

Handran SD, Werth JL, DeVivo DC, Rothman SM. Mitochondrial morphology and intracellular calcium homeostasis in cytochrome oxidase-deficient human fibroblasts. Neurobiology of disease. 1997; 3:287–298. [PubMed: 9173926]

Head B, Griparic L, Amiri M, Gandre-Babbe S, van der Bliek AM. Inducible proteolytic inactivation of OPA1 mediated by the OMA1 protease in mammalian cells. J Cell Biol. 2009; 187:959–966. [PubMed: 20038677]

Herlan M, Vogel F, Bornhovd C, Neupert W, Reichert AS. Processing of Mgm1 by the rhomboid-type protease Pcp1 is required for maintenance of mitochondrial morphology and of mitochondrial DNA. J Biol Chem. 2003; 278:27781–27788. [PubMed: 12707284]

Hermann GJ, Thatcher JW, Mills JP, Hales KG, Fuller MT, Nunnari J, Shaw JM. Mitochondrial fusion in yeast requires the transmembrane GTPase Fzo1p. J Cell Biol. 1998; 143:359–373. [PubMed: 9786948]

Hoppins S, Edlich F, Cleland MM, Banerjee S, McCaffery JM, Youle RJ, Nunnari J. The soluble form of Bax regulates mitochondrial fusion via MFN2 homotypic complexes. Molecular cell. 2011; 41:150–160. [PubMed: 21255726]

Huckriede A, Heikema A, Sjollema K, Briones P, Agsteribbe E. Morphology of the mitochondria in heat shock protein 60 deficient fibroblasts from mitochondrial myopathy patients. Effects of stress conditions. Virchows Archiv : an international journal of pathology. 1995; 427:159–165. [PubMed: 7582246]

Ishihara N, Fujita Y, Oka T, Mihara K. Regulation of mitochondrial morphology through proteolytic cleavage of OPA1. The EMBO journal. 2006; 25:2966–2977. [PubMed: 16778770]

Karbowski M, Arnoult D, Chen H, Chan DC, Smith CL, Youle RJ. Quantitation of mitochondrial dynamics by photolabeling of individual organelles shows that mitochondrial fusion is blocked during the Bax activation phase of apoptosis. J Cell Biol. 2004; 164:493–499. [PubMed: 14769861]

Kaser M, Kambacheld M, Kisters-Woike B, Langer T. Oma1, a novel membrane-bound metallopeptidase in mitochondria with activities overlapping with the m-AAA protease. J Biol Chem. 2003; 278:46414–46423. [PubMed: 12963738]

Koopman WJ, Visch HJ, Verkaart S, van den Heuvel LW, Smeitink JA, Willems PH. Mitochondrial network complexity and pathological decrease in complex I activity are tightly correlated in isolated human complex I deficiency. American journal of physiology Cell physiology. 2005; 289:C881–890. [PubMed: 15901599]

Kwong JQ, Henning MS, Starkov AA, Manfredi G. The mitochondrial respiratory chain is a modulator of apoptosis. J Cell Biol. 2007; 179:1163–1177. [PubMed: 18086914]

Langklotz S, Baumann U, Narberhaus F. Structure and function of the bacterial AAA protease FtsH. Biochimica et biophysica acta. 2012; 1823:40–48. [PubMed: 21925212]

Legros F, Lombes A, Frachon P, Rojo M. Mitochondrial fusion in human cells is efficient, requires the inner membrane potential, and is mediated by mitofusins. Mol Biol Cell. 2002; 13:4343–4354. [PubMed: 12475957]

Malka F, Guillery O, Cifuentes-Diaz C, Guillou E, Belenguer P, Lombes A, Rojo M. Separate fusion of outer and inner mitochondrial membranes. EMBO Rep. 2005; 6:853–859. [PubMed: 16113651]

Meeusen S, McCaffery JM, Nunnari J. Mitochondrial fusion intermediates revealed in vitro. Science. 2004; 305:1747–1752. [PubMed: 15297626]

Meeusen S, DeVay R, Block J, Cassidy-Stone A, Wayson S, McCaffery JM, Nunnari J. Mitochondrial inner-membrane fusion and crista maintenance requires the dynamin-related GTPase Mgm1. Cell. 2006; 127:383–395. [PubMed: 17055438]

Quiros PM, Ramsay AJ, Sala D, Fernandez-Vizarra E, Rodriguez F, Peinado JR, Fernandez-Garcia MS, Vega JA, Enriquez JA, Zorzano A, et al. Loss of mitochondrial protease OMA1 alters processing of the GTPase OPA1 and causes obesity and defective thermogenesis in mice. The EMBO journal. 2012; 31:2117–2133. [PubMed: 22433842]

Rogers GW, Brand MD, Petrosyan S, Ashok D, Elorza AA, Ferrick DA, Murphy AN. High throughput microplate respiratory measurements using minimal quantities of isolated mitochondria. PloS one. 2011; 6:e21746. [PubMed: 21799747]

Rossignol R, Gilkerson R, Aggeler R, Yamagata K, Remington SJ, Capaldi RA. Energy substrate modulates mitochondrial structure and oxidative capacity in cancer cells. Cancer research. 2004; 64:985–993. [PubMed: 14871829]

Santo-Domingo J, Giacomello M, Poburko D, Scorrano L, Demaurex N. OPA1 promotes pH flashes that spread between contiguous mitochondria without matrix protein exchange. The EMBO journal. 2013; 32:1927–1940. [PubMed: 23714779]

Sauvanet C, Duvezin-Caubet S, di Rago JP, Rojo M. Energetic requirements and bioenergetic modulation of mitochondrial morphology and dynamics. Seminars in cell & developmental biology. 2010; 21:558–565.

Sauvanet C, Duvezin-Caubet S, Salin B, David C, Massoni-Laporte A, di Rago JP, Rojo M. Mitochondrial DNA mutations provoke dominant inhibition of mitochondrial inner membrane fusion. PloS one. 2012; 7:e49639. [PubMed: 23166736]

Schauss AC, Huang H, Choi SY, Xu L, Soubeyrand S, Bilodeau P, Zunino R, Rippstein P, Frohman MA, McBride HM. A novel cell-free mitochondrial fusion assay amenable for high-throughput screenings of fusion modulators. BMC biology. 2010; 8:100. [PubMed: 20659315]

Song Z, Chen H, Fiket M, Alexander C, Chan DC. OPA1 processing controls mitochondrial fusion and is regulated by mRNA splicing, membrane potential, and Yme1L. J Cell Biol. 2007; 178:749–755. [PubMed: 17709429]

Song Z, Ghochani M, McCaffery JM, Frey TG, Chan DC. Mitofusins and OPA1 mediate sequential steps in mitochondrial membrane fusion. Mol Biol Cell. 2009; 20:3525–3532. [PubMed: 19477917]

Stiburek L, Cesnekova J, Kostkova O, Fornuskova D, Vinsova K, Wenchich L, Houstek J, Zeman J. YME1L controls the accumulation of respiratory chain subunits and is required for apoptotic resistance, cristae morphogenesis, and cell proliferation. Mol Biol Cell. 2012; 23:1010–1023. [PubMed: 22262461]

Westermann B. Mitochondrial fusion and fission in cell life and death. Nat Rev Mol Cell Biol. 2010; 11:872–884. [PubMed: 21102612]

Youle RJ, van der Bliek AM. Mitochondrial fission, fusion, and stress. Science. 2012; 337:1062–1065. [PubMed: 22936770]

HIGHLIGHTS

- Mitochondrial inner membrane fusion is stimulated by oxidative phosphorylation.
- Cleavage of Opa1 by Yme1L couples inner membrane fusion to metabolism.
- Opa1 cleavage stimulates mitochondrial inner membrane fusion.
- Diseases of mtDNA disrupt the linkage of oxidative phosphorylation to fusion.

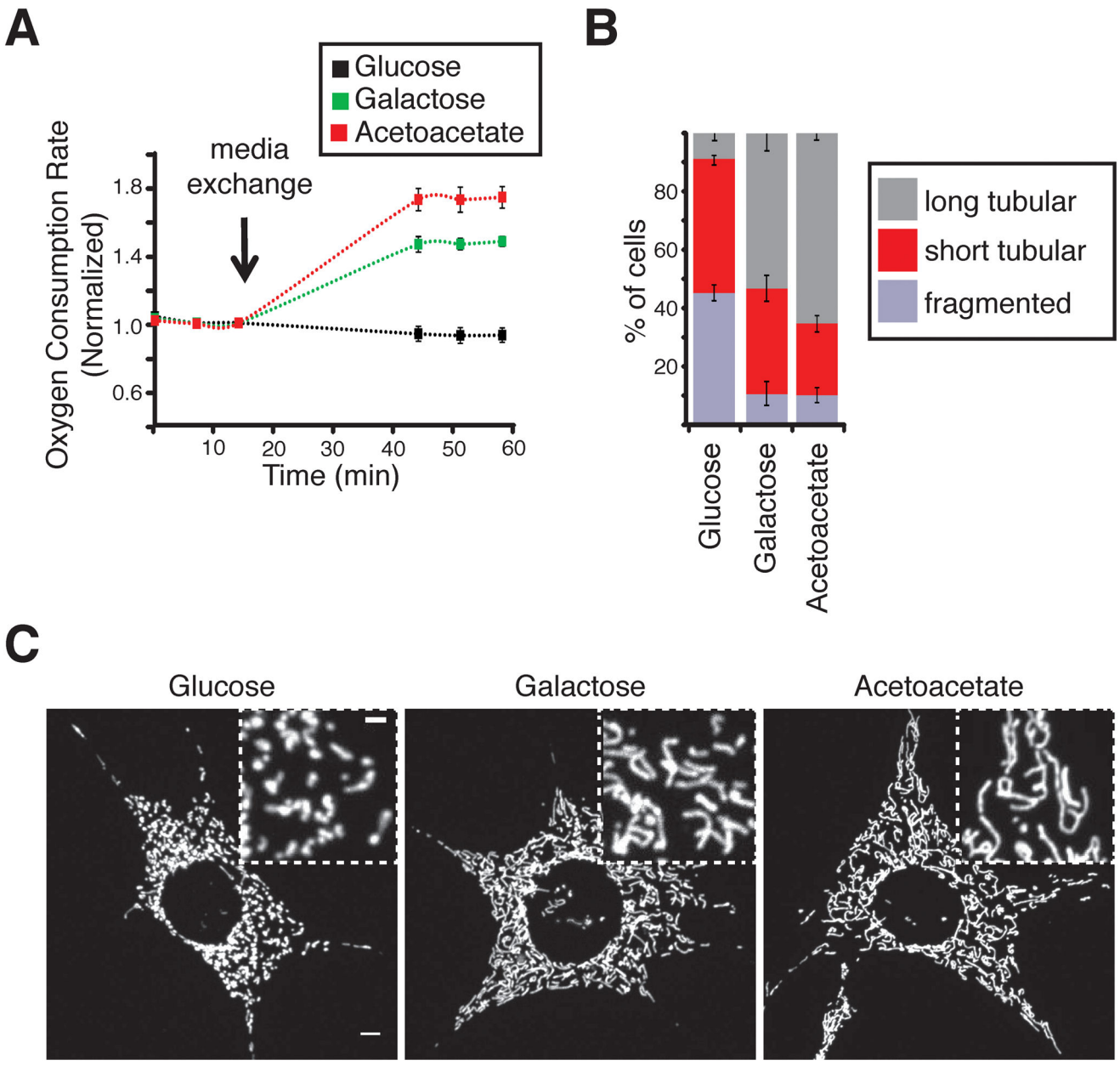

Figure 1. Oxidative conditions stimulate mitochondrial fusion

(A) Inducing oxygen consumption with oxidative media. MEFs were grown in glucose-containing media and then switched to glucose, galactose or acetoacetate containing media. Error bars indicate standard deviations. **(B)** Quantitation of mitochondrial morphology at 24 hours after media shift. Cells were classified as having mostly fragmented mitochondria, short tubular mitochondria or long tubular mitochondria. Error bars indicate standard deviations. **(C)** Representative images of mitochondrial morphology (matrix-targeted DsRed) at 24 hours after media shift. Scale bar, 5 μm.

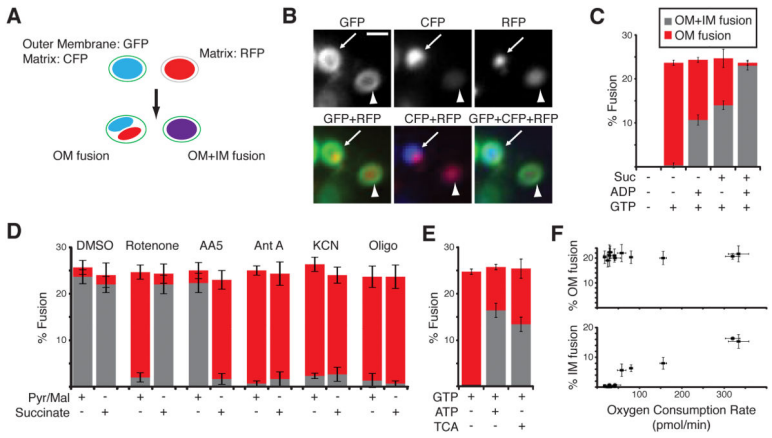

Figure 2. OXPHOS stimulates inner membrane fusion *in vitro*

(A) Schematic of the *in vitro* fusion assay. Mitochondria containing OM-targeted GFP and matrix CFP were mixed with mitochondria containing matrix RFP. Full fusion events (both OM and IM fusion) are indicated by colocalized CFP and RFP matrices that are surrounded by a single GFP membrane. OM fusion intermediates are indicated by apposed but distinct CFP and RFP matrices that are surrounded by a single GFP membrane. **(B)** Image of an *in vitro* fusion reaction showing unfused mitochondria, OM fusion intermediates (arrow), and full fusion events (arrowhead). Scale bar, 1 μm. **(C)** Dependence of OM and IM *in vitro* fusion events on respiratory substrates. Events are plotted as percentage of total mitochondria. **(D)** Sensitivity of *in vitro* fusion to ETC inhibition in respiratory conditions. ADP and GTP are present in all reactions. Pyruvate, malate (‘Pyr/Mal’, complex I substrates) or succinate (complex II substrate) was added as indicated. The following drugs were tested: rotenone (complex I inhibitor), atpenin A5 (AA5, complex II inhibitor), antimycin A (Ant A, complex III inhibitor), potassium cyanide (KCN, complex IV inhibitor), and oligomycin (oligo, complex V inhibitor). Same color schemes as (C). **(E)** Partial support of *in vitro* fusion events by ATP or the tricarboxylic acid cycle. Same color scheme as (C). GTP and ATP were added as indicated. TCA: substrates for the tricarboxylic acid cycle (α-ketoglutarate, aspartate, NADH). **(F)** OM (top) and IM (bottom) fusion rates *in vitro* as a function of oxygen consumption rate. All error bars indicate standard deviation.

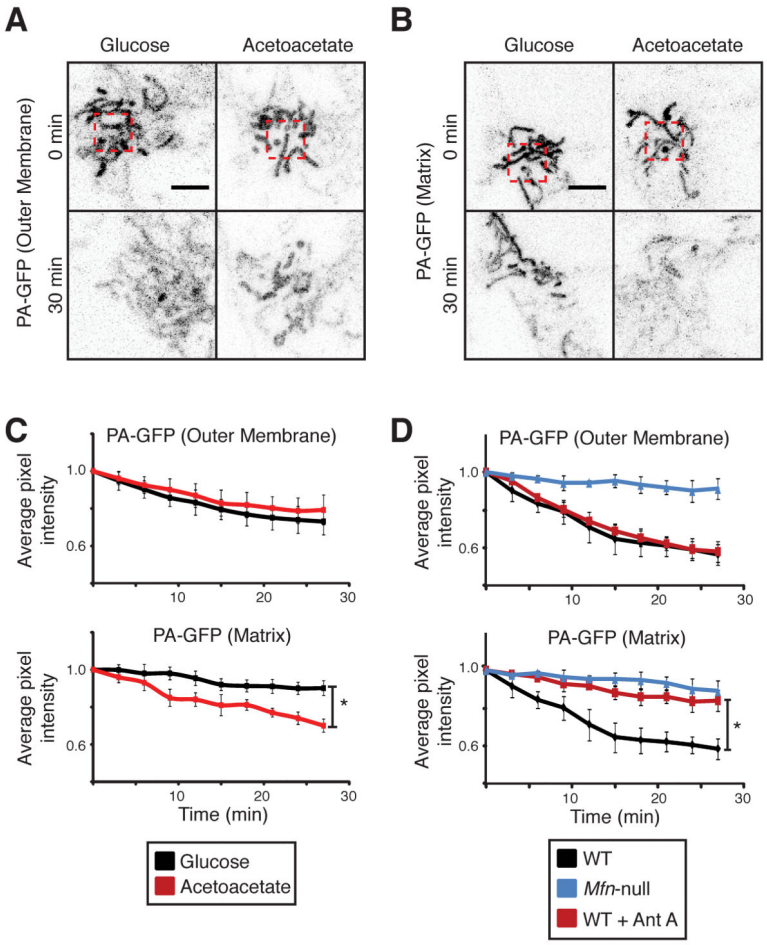

Figure 3. Inner membrane fusion is inhibited under glycolytic conditions *in vivo*

(A) OM fusion in wildtype MEFs. At time t=0 min, PA-GFP in the OM was activated in a region of interest (red box). Dilution of the PA-GFP signal was followed every 3 min for 30 min. Representative images at 0 min and 30 min are shown. Scale bar, 5 μm. **(B)** IM fusion in wildtype MEFs. Same as in (**A**), but using PA-GFP targeted to the matrix. Scale bar, 5 μm. **(C)** OM and IM fusion rates *in vivo* in glycolytic and oxidative media, measured by dilution of PA-GFP. The p-values were calculated for the slopes (pixel intensity versus time) using the Student's t-test. **(D)** OM and IM fusion rates *in vivo* in the presence and absence of the complex III inhibitor antimycin A (Ant A). As a negative control, data from mitofusin-deficient MEFs (Mfn: *Mfn1* −/−, *Mfn2* −/−) are shown. The p-values were calculated as in (C). All error bars indicate standard deviations. *p < 0.01.

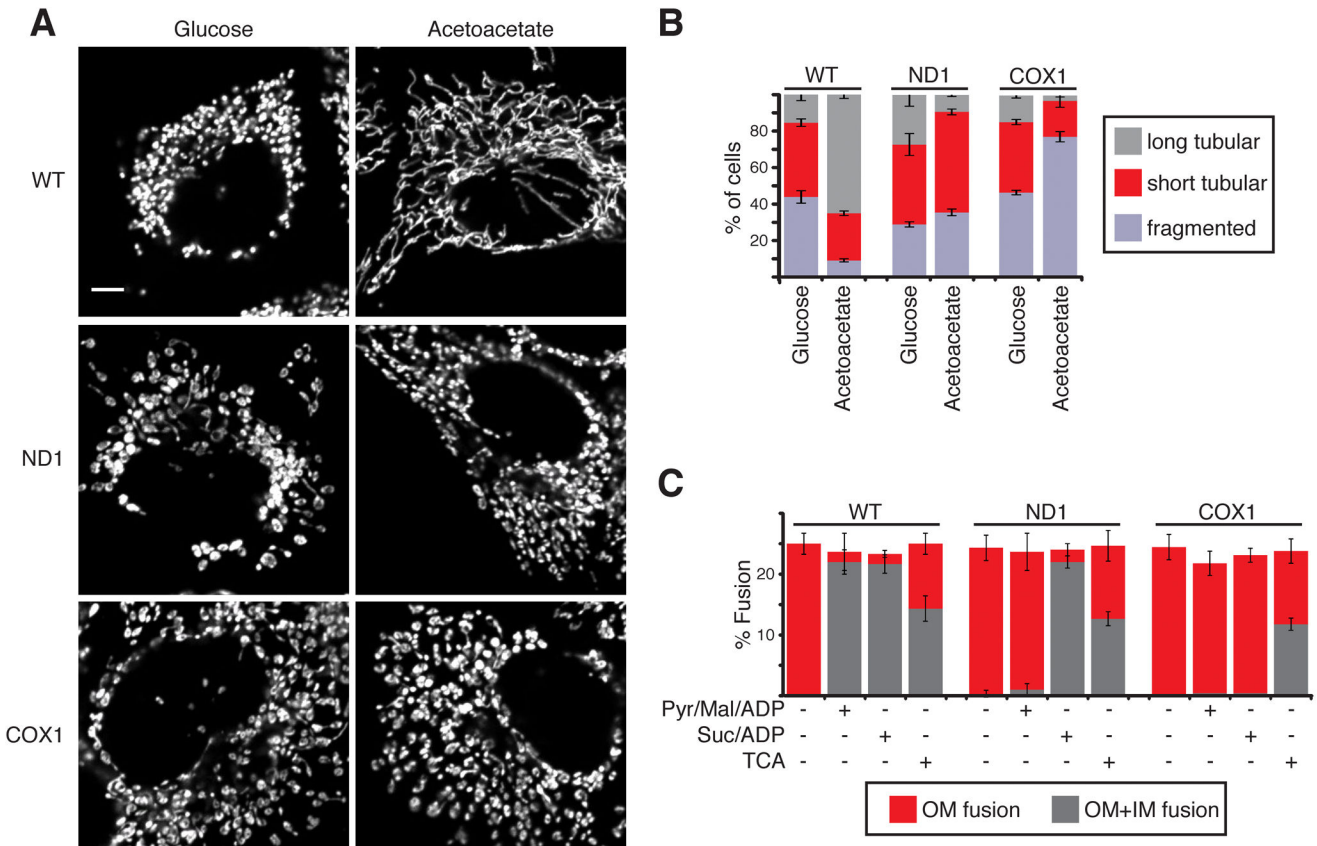

Figure 4. Pathogenic mtDNA mutations impair OXPHOS-driven IM fusion

(A) Failure of ND1 (complex I mutant) and COXI (complex IV mutant) cells to elongate mitochondria when shifted to oxidative media for 4 hours. Mitochondria were visualized via expression of matrix-targeted DsRed. Scale bar, 5 μm. **(B)** Quantification of mitochondrial morphology in wildtype and mutant cells in glycolytic ("Glucose") versus oxidative ("Acetoacetate") media. **(C)** Defective IM fusion *in vitro* in mitochondria of mutant cells. All reactions contain GTP. Pyr, pyruvate; Mal, malate; Suc, succinate; TCA: substrates for the tricarboxylic acid cycle (α-ketoglutarate, aspartate, NADH). All error bars indicate standard deviations.

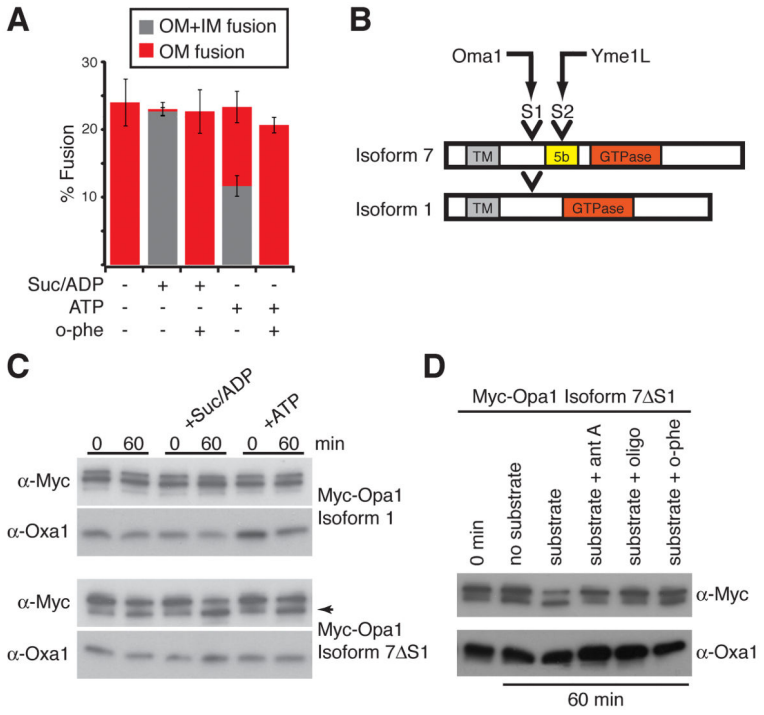

Figure 5. Opa1 processing at site S2 is necessary for OXPHOS-induced fusion

(A) Inhibition of IM fusion events *in vitro* by o-phenanthroline. All reactions contain GTP. Suc, succinate; o-phe, o-phenanthroline. Error bars indicate standard deviations. **(B)** Schematic of Opa1 mRNA splice forms 1 and 7, showing locations of the S1 and S2 cleavage sites. **(C)** Processing at the S1 (top two panels) and S2 (bottom two panels) sites of myc-Opa1 *in vitro* in response to respiratory conditions or ATP. Oxa1 levels are shown as a control. Processing to the short form of myc-Opa1 isoform 7ΔS1 (arrow) occurs in response to respiratory conditions. **(D)** Processing at the Opa1 S2 site *in vitro* in response to ETC inhibition. Substrate (succinate, ADP) and drugs [antimycin A (ant A), oligomycin (oligo) and o-phenanthroline (o-phe)] were added as indicated.

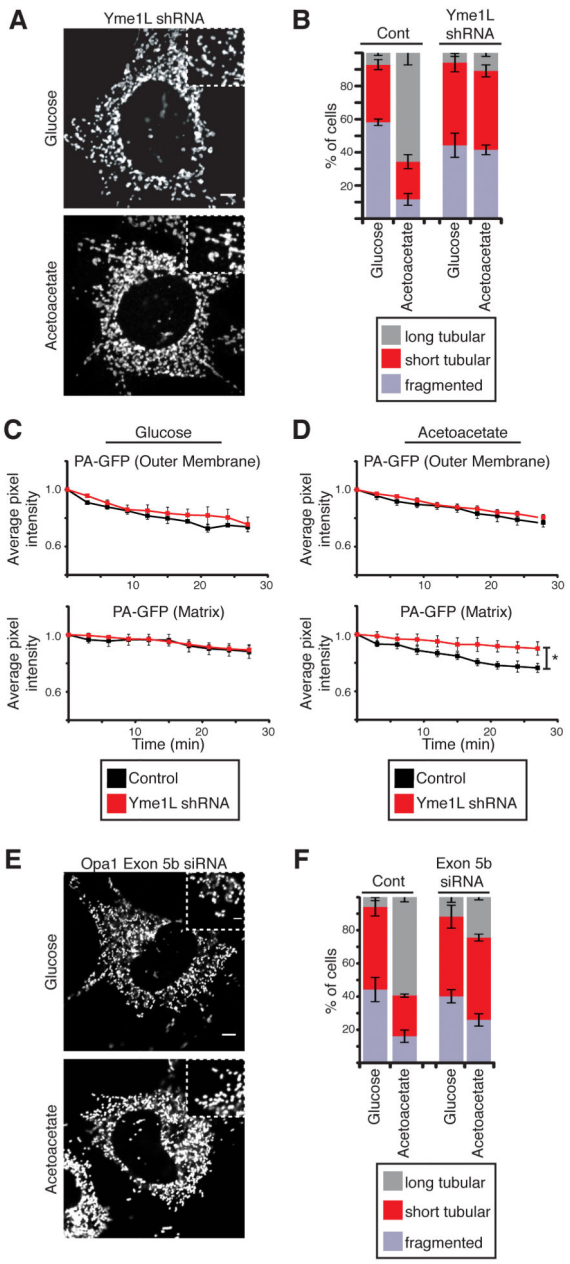

Figure 6. Yme1L is necessary for OXPHOS-induced fusion

(A) Representative images of mitochondrial morphology in Yme1L-depleted MEFs at 24 hours after shifting to glycolytic (top) or oxidative (bottom) media. Mitochondria were visualized via staining for Tom20, a mitochondrial outer membrane protein. Scale bar, 5 μm. **(B)** Quantification of mitochondrial morphology in control and Yme1L-depleted cells in glycolytic ("Glucose") versus oxidative ("Acetoacetate") media. **(C)** OM fusion rates (top) and IM fusion rates (bottom) measured by PA-GFP dilution *in vivo* under glycolytic conditions. Yme1L-knockdown cells are compared with control cells. **(D)** Same as (C), but under oxidative conditions. The p-values were calculated for the slopes (pixel intensity versus time) using the Student's t-test. *$p < 0.01$. **(E)** Representative images of

mitochondrial morphology in exon 5b knockdown cells after shifting to glycolytic ("Glucose") or oxidative ("Acetoacetate") media for 24 hours. Mitochondria were visualized via staining for Tom20, a mitochondrial OM protein. Scale bar, 5 μm. **(F)** Quantitation of mitochondrial morphology in control and exon 5b-depleted cells in glycolytic and oxidative media. All error bars indicate standard deviations.

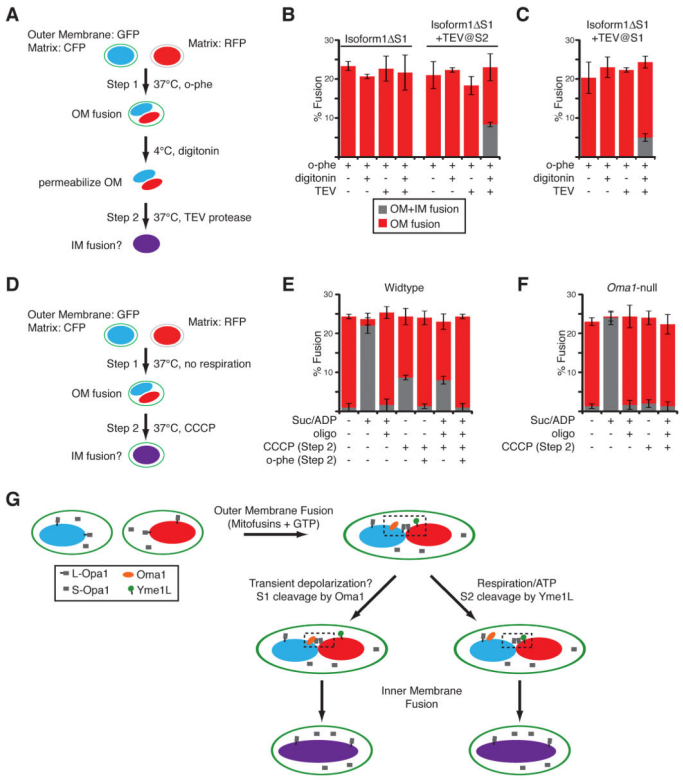

Figure 7. Induced proteolytic processing of Opa1 promotes inner membrane fusion

(A) Schematic of the *in vitro* fusion experiment in (B) and (C). o-phenanthroline is present throughout, and digitonin and TEV protease are added after OM fusion. **(B)** Induction of IM fusion by engineered cleavage at S2. OM and IM fusion events in mitochondria containing Opa1 lacking a TEV site (1ΔS1) or containing a TEV site at the S2 position (1ΔS1 + TEV@S2). In the latter, S2 cleavage was controlled by addition of digitonin and TEV. **(C)** Induction of IM fusion by engineered cleavage at S1. The experiment is similar to (B), but using an Opa1 isoform containing a TEV site at the S1 position. Same color scheme as (B). (**D**) Schematic of the *in vitro* fusion experiment in (E) and (F). Isolated mitochondria are allowed to proceed through OM fusion (Step 1) in the absence of respiration. CCCP is then added to induce Opa1 processing at S1 (Step 2). **(E)** Induction of IM fusion by CCCP. OM and IM fusion events in wild-type mitochondria after CCCP-induced processing of Opa1. Suc, succinate; o-phe, o-phenanthroline; oligo, oligomycin. Same color scheme as (B). **(F)** Same as (E), except using *Oma1*-null mitochondria. All error bars indicate standard deviations. **(G)** Model for activation of Opa1 and IM fusion by proteolysis. OM fusion is permissive, as long as mitofusins and GTP are present. In contrast, IM fusion is regulated by the Yme1L or Oma1 metalloproteases, which acutely cleave long isoforms of Opa1 (L-Opa1) as part of the fusion mechanism. Yme1L activity is regulated by mitochondrial respiration and/or ATP levels, while Oma1 activity is potentially regulated by transient IM depolarizations.